JOURNAL OF MATERIALS SCIENCE 16 (1981) 569–578

Review
Electrostrictive effect in perovskites and its transducer applications

KENJI UCHINO, SHOICHIRO NOMURA
Department of Physical Electronics, Tokyo Institute of Technology, Ookayama, Meguro-ku, Tokyo 152, Japan

LESLIE E. CROSS, ROBERT E. NEWNHAM, SEI J. JANG
Materials Research Laboratory, The Pennsylvania State University, University Park, Pennsylvania 16802, USA

Properties of new electrostrictive materials for displacive transducers are reviewed including theoretical, material and design studies. Intensive investigation of the electrostrictive effects in ferroelectric and antiferroelectric perovskites have led to some empirical rules: the product of the electrostriction coefficient Q and the Curie–Weiss constant C is constant for all perovskite crystals and the Q value is proportional to the square of the thermal expansion coefficient, α. Consistent with the empirical rules, the relaxor ferroelectric ceramic 0.9 $Pb(Mg_{1/3}Nb_{2/3})O_3$–0.1 $PbTiO_3$ possesses much larger strain with lower hysteresis, aging effects and thermal expansion than that obtained with piezoelectric lead zirconate titanate (PZT). Using a multilayer configuration similar to commercial capacitors, a new mirror control device capable of large strains with high reproducibility, up to $\Delta L/L \sim 10^{-3}$, with only 200 V applied has been developed.

1. Introduction

Electrostriction, the basic electromechanical coupling in all non-piezoelectric solids, is at present very poorly understood. There are few reliable measurements of the electrostriction tensor components, even in simple solids. The principal difficulty is associated with the small magnitude of the electrostrictive strains even at very high field levels. Theoretically, the absence of well authenticated experimental values has certainly been a major disincentive to development, and none of the present theories are viable.

The introduction of new displacive transducers to control optical beams in astronomy and communication have, however, prompted the development of a new family of electrostrictive ceramics. Properties which are important in materials for displacement transducers are as follows:

(1) Sensitivity (strain/electric field);
(2) Reproducibility (hysteresis);
(3) Stability (temperature, aging);
(4) Response time, resonances, damping;
(5) Dielectric strength, resistivity;
(6) Availability (size, weight).

The initial choices of materials were magnetostrictive or piezoelectric. Magnetostriction is not very useful because the strains ($\Delta L/L \sim 10^{-5}$–10^{-4}) are much smaller than in piezoelectric materials ($\Delta L/L \sim 10^{-4}$–10^{-2}) and because of the necessity of a large driving coil. The problems with piezoelectric ceramics are a large hysteresis and a substantial aging effect. On the other hand, the electrostriction in non-ferroic crystals is not associated with hysteresis or aging, and the response time is much faster than that of domain reorientations in ferroelectrics. An additional merit is that electric poling is not required. To take advantage of these characteristics new materials are needed with "enormous" electrostriction, contrary to the usual conception!

In this paper we review the properties of new electrostrictive transducers developed in

0022–2461/81/030569–10$03.00/0

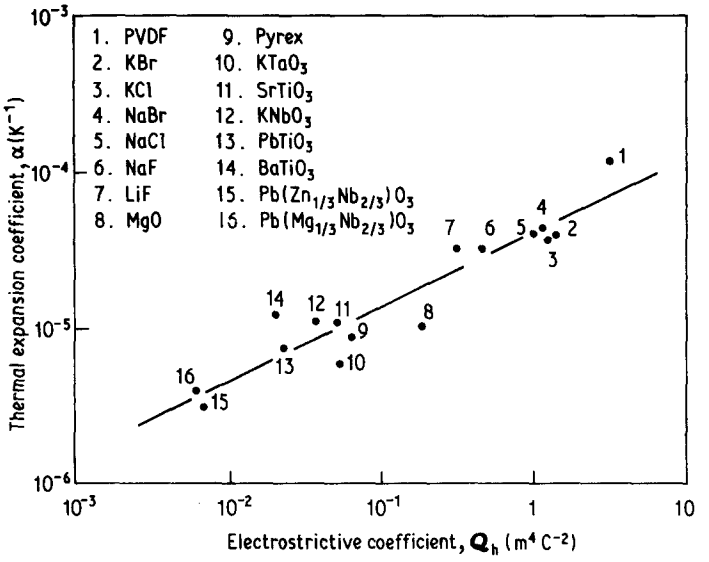

Figure 1 Thermal expansion coefficient α plotted as a function of hydrostatic electrostriction coefficient Q_h for various materials. The straight line has a slope of 0.5.

co-operative work at the Tokyo Institute of Technology and The Pennsylvania State University, including theoretical, material and design studies.

2. Electrostriction and its interrelation with with thermal expansion

Electrostriction is a measure of the electric field (or polarization) induced shifts of the atoms or ions away from their natural equilibrium positions. Induced shifts of equivalent atoms or ions almost cancel each other in centric crystals, and only the shift difference due to potential anharmonicity causes strain. The electrostriction coefficients Q (or M) are defined as coefficients in the relationship between electric polarization, **P**, (or field **E**) and observed elastic strain **x**, expressed as $\mathbf{x} = Q\mathbf{P}^2$ (or $M\mathbf{E}^2$). Clearly, since the strain is a second rank polar tensor and **E** and **P** are polar vectors, then Q or M are fourth rank polar tensors. In a similar manner, the thermal expansion coefficient, α, can be regarded as a "compliance" coefficient defined by the relationship of strain with temperature T ($\Delta L/L = \alpha T$).

It is thus not unreasonable to expect that these anharmonicity related "compliance" coefficients will be interrelated. In Fig. 1, the thermal expansion coefficient α is plotted against the hydrostatic electrostriction coefficient $Q_h(= Q_{11} + 2Q_{12})$ for the materials of isotropic or cubic symmetry. Sources of the experimental data are listed in reference [1]. The power relation

$$\alpha = 4.2 \times 10^{-5} Q_h^{0.5} \qquad (1)$$

was obtained for this graph.

3. Phenomenology of electrostriction

3.1. Case of ferroelectrics

First the thermodynamic phenomenology of electrostriction in ferroelectrics will be reviewed. Detailed treatments of this effect can be found in the papers of Devonshire [2], Kay [3] and Forsbergh [4]. For convenience, take the elastic Gibbs energy $G_1(X, \mathbf{P}, T)(\mathrm{d}G_1 = x_{ij}\,\mathrm{d}X_{ij} + \mathbf{E}_m\,\mathrm{d}\mathbf{P}_m - S\mathrm{d}T)$ as the thermodynamical function where S is entropy. The free energy, G_1, can be expressed as a polynomial in electric polarization **P** and stress X

$$\begin{aligned} G_1 = {} & \tfrac{1}{2}\alpha_{ij}P_iP_j + \tfrac{1}{4}\beta_{ijkl}P_iP_jP_kP_l \\ & + \tfrac{1}{6}\gamma_{ijklmn}P_iP_jP_kP_lP_mP_n \\ & - \tfrac{1}{2}s_{ijkl}X_{ij}X_{kl} \\ & - Q_{ijkl}P_iP_jX_{kl}. \end{aligned} \qquad (2)$$

The subscripts denote directional tensor components.

Using the Voigt notation, the electrostriction coefficient tensor Q_{ij} is defined in a stress-free cubic crystal ($X = 0$) by the following equation

$$\begin{pmatrix} x_1 \\ x_2 \\ x_3 \\ x_4 \\ x_5 \\ x_6 \end{pmatrix} = \begin{pmatrix} Q_{11} & Q_{12} & Q_{12} & 0 & 0 & 0 \\ Q_{12} & Q_{11} & Q_{12} & 0 & 0 & 0 \\ Q_{12} & Q_{12} & Q_{11} & 0 & 0 & 0 \\ 0 & 0 & 0 & Q_{44} & 0 & 0 \\ 0 & 0 & 0 & 0 & Q_{44} & 0 \\ 0 & 0 & 0 & 0 & 0 & Q_{44} \end{pmatrix} \begin{pmatrix} P_1^2 \\ P_2^2 \\ P_3^2 \\ P_2P_3 \\ P_3P_1 \\ P_1P_2 \end{pmatrix}. \qquad (3)$$

These equations suggest one way of determining the electrostriction coefficients: by comparing the field or the polarization with the resulting strain. Note that the polarization can be either induced or spontaneous, corresponding to an induced or spontaneous strain, respectively. Therefore, the spontaneous volume change $(\Delta V/V)_s$ at the transition temperature can be written as

$$(\Delta V/V)_s = Q_h \mathbf{P}_s^2, \tag{4}$$

where $Q_h = Q_{11} + 2Q_{12}$ and $\mathbf{P}_s^2 (= P_1^2 + P_2^2 + P_3^2)$ is the spontaneous polarization at the Curie temperature.

Another way of determining the coefficients is obtained from the following argument. When a hydrostatic pressure, p, is applied to a centrosymmetric paraelectric crystal, the reciprocal dielectric susceptibility, χ_1, is derived from the free energy G_1 as

$$\chi_1 = \alpha_1 + 2Q_h \mathbf{P}, \tag{5}$$

where $\alpha_1 = (T - T_0)/C$ (Curie–Weiss law), T_0 is the Curie–Weiss temperature, and C the Curie–Weiss constant. The hydrostatic electrostriction coefficient Q_h is a measure of the rate of variation of the reciprocal susceptibility with pressure.

The values of the electrostriction coefficients can also be checked by using the shift of transition temperature, T_c, or Curie–Weiss temperature, T_0, with hydrostatic pressure, derived from Equation 6

$$(\partial T_0/\partial p) = (\partial T_c/\partial p) = -2Q_h C. \tag{6}$$

3.2. Case of antiferroelectrics

Electrostrictive terms have been introduced into the Kittel free energy expression [5] for antiferroelectrics in reference [6] as follows

$$\begin{aligned} G_1 = {} & \tfrac{1}{2}\alpha(T)(\mathbf{P}_a^2 + \mathbf{P}_b^2) + \tfrac{1}{4}\beta(\mathbf{P}_a^4 + \mathbf{P}_b^4) \\ & + \tfrac{1}{6}\gamma(\mathbf{P}_a^6 + \mathbf{P}_b^6) + \eta \mathbf{P}_a \mathbf{P}_b - \tfrac{1}{2}\chi_T p^2 \\ & + Q_h(\mathbf{P}_a^2 + \mathbf{P}_b^2 + 2\Omega \mathbf{P}_a \mathbf{P}_b)p. \end{aligned} \tag{7}$$

This is a one-dimensional expression in which $\mathbf{P}_a$ and $\mathbf{P}_b$ denote the two sublattice polarizations, p is the hydrostatic pressure, χ_T the isothermal compressibility, and Q_h and Ω are electrostriction coefficients. An additional coefficient Ω is required to take account of the interaction between the sublattice polarizations. Introducing the Cross transformations [7] $\mathbf{P}_F = (\mathbf{P}_a + \mathbf{P}_b)/2^{1/2}$ and $\mathbf{P}_A = (\mathbf{P}_a - \mathbf{P}_b)/2^{1/2}$ leads to the following results.

Above the transition temperature the induced volume change is related to the induced ferroelectric polarization by

$$(\Delta V/V)_i = Q_h(1 + \Omega)\mathbf{P}_{F,i}^2, \tag{8}$$

while below the Néel temperature the spontaneous volume change is related to the spontaneous antiferroelectric polarization by

$$(\Delta V/V)_s = Q_h(1 - \Omega)\mathbf{P}_{A,s}^2. \tag{9}$$

In the case of antiferroelectrics, the spontaneous volume change at the transition temperature can be either positive or negative, depending on the Ω values, which differs markedly from ferroelectrics.

The pressure derivatives of the Néel and Curie–Weiss temperature are

$$(\partial T_N/\partial p) = -2Q_h(1 - \Omega)C \tag{10}$$

and

$$(\partial T_0/\partial p) = -2Q_h(1 + \Omega)C, \tag{11}$$

where C is the Curie–Weiss constant. The variation of the reciprocal susceptibility, χ, with hydrostatic pressure in the paraelectric phase is

$$(\partial \chi/\partial p) = 2Q_h(1 + \Omega). \tag{12}$$

Good agreement between the experimental data [8, 9] and the predictions has been obtained for the antiferroelectric perovskites $PbZrO_3$ and $Pb(Mg_{1/2}W_{1/2})O_3$.

4. Experimental methods of measuring electrostriction

As suggested in the previous section, there are several experimental methods for determining the electrostriction coefficients. Direct measurements of strain include optical methods (interferometer and optical lever), X-ray methods, electrical methods (capacitance and differential transformer), and strain gauge methods. Pressure gauge methods and the pressure dependence of the dielectric permittivity are indirect measurements. Some experimental measurements on the relaxor ferroelectric perovskite $Pb(Mg_{1/3}Nb_{2/3})O_3$ are discussed in the following sections.

4.1. Strain gauge methods [10]

Fig. 2 shows a strain gauge determination of longitudinal electrostrictive strain σ_1 measured as a function of an applied electric field (0.002 Hz) at various temperatures between -10 and $+80^\circ$ C. Experimental values of the electrostriction coefficients are plotted as a function of temperature in

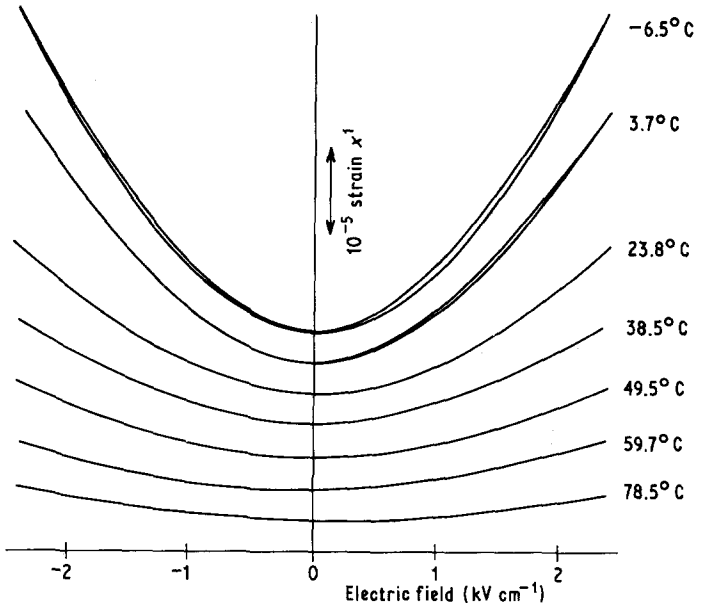

Figure 2 Electric field dependence of the longitudinal electrostriction in $Pb(Mg_{1/3}Nb_{2/3})O_3$ at various temperatures (Strain gauge methods).

Fig. 3. It is evident that the electrostriction coefficients do not change significantly through the relaxation temperature range

$$(Q_{11} = 2.50(\pm 0.14) \times 10^{-2}\,m^4C^{-2},$$
$$Q_{12} = -0.96(\pm 0.02) \times 10^{-2}\,m^4C^{-2}).$$

4.2. Pressure dependence of permittivity [10]

Fig. 4 shows the variation of the reciprocal susceptibility with hydrostatic pressure at various temperatures. The gradual increase in slope observed for $Pb(Mg_{1/3}Nb_{2/3})O_3$ with increasing temperature, can be explained by the diffuse phase transition theory. Using Equation 6 the hydrostatic electrostriction coefficient Q_h can be calculated as $0.60(\pm 0.08) \times 10^{-2}\,m^4C^{-2}$, in good agreement with the value calculated from the direct electro-

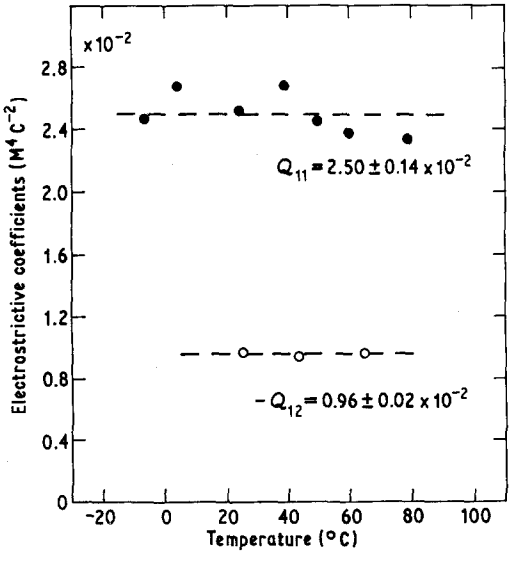

Figure 3 Temperature dependence of the electrostriction in $Pb(Mg_{1/3}Nb_{2/3})O_3$ single crystals.

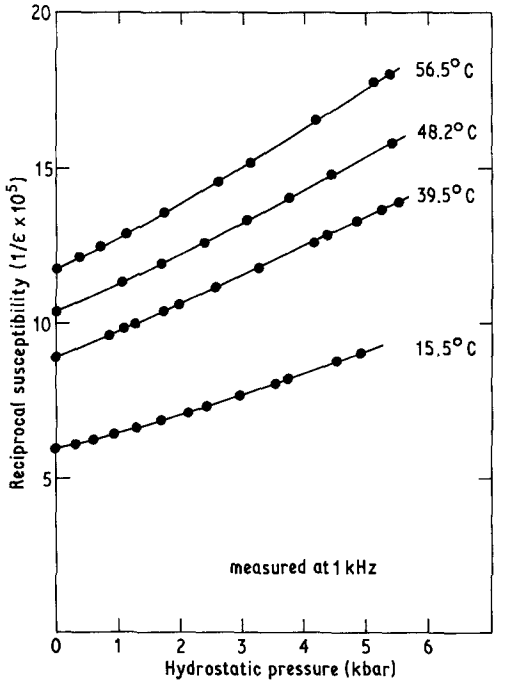

Figure 4 Hydrostatic pressure dependence of the reciprocal permittivity in $Pb(Mg_{1/3}Nb_{2/3})O_3$ at various temperatures.

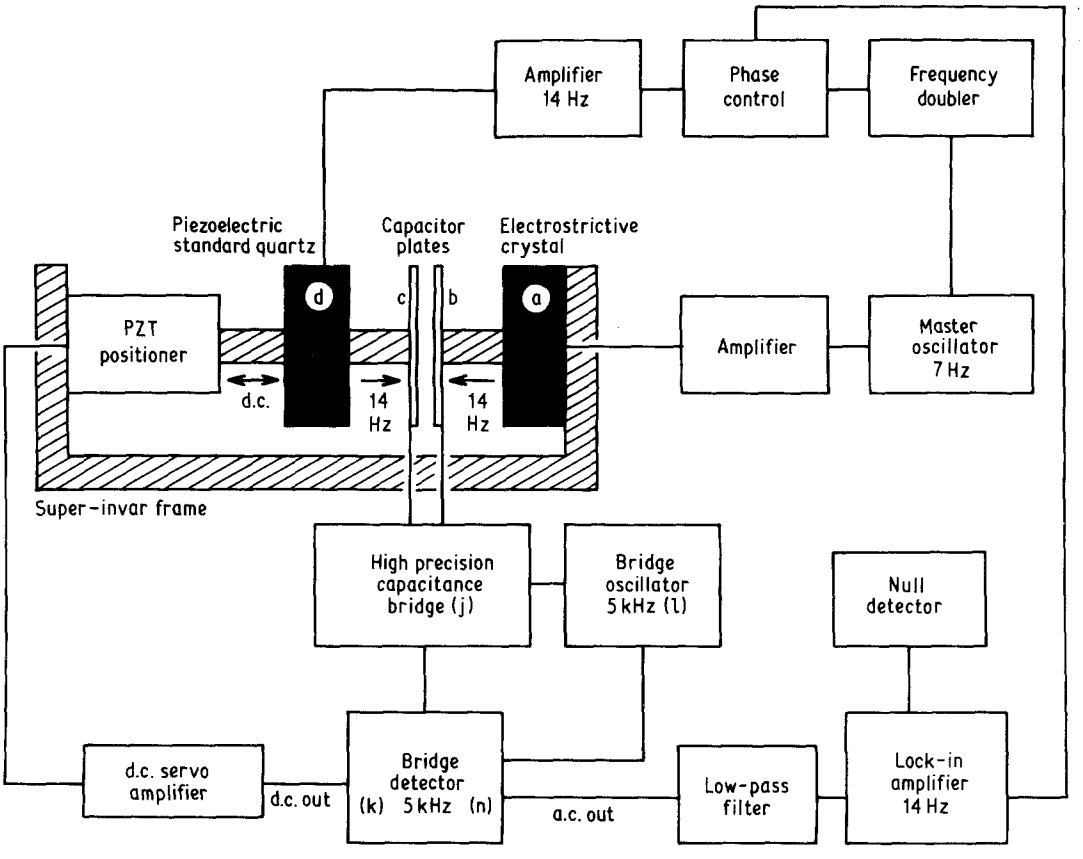

Figure 5 Schematic diagram of the a.c. capacitance dilatometer.

strictive strain measurements ($Q_{11} + 2Q_{12} = 0.58(\pm 0.18) \times 10^{-2}\,m^4C^{-2}$).

4.3. A.c. capacitance dilatometer [11, 12]

A new type of ultrasensitive capacitance dilatometer especially suited to low permittivity solids has been constructed which is capable of resolving low frequency a.c. linear displacements of 10^{-13}m(10^{-3}Å) (Fig. 5). To measure the electrostriction coefficient, an electric field at 7 Hz is applied to the sample crystal through an oscillator amplifier combination. This sets the sensing capacitor plate vibrating at 14 Hz. A phase locked signal at 14 Hz is then applied to the standard quartz crystal. The lock-in amplifier which is phase-locked to the 14 Hz driving frequency senses any component in the bridge output (capacitance) which is at 14 Hz and in phase with the driving oscillator. By manipulating voltages applied to the unknown and standard crystals, a null condition can be achieved. The unknown coefficient can then be derived from the voltage ratio and appropriate geometrical constants. Thermal drift causes a change in the separation of the capacitor plates, resulting in a d.c. unbalance at the bridge. This signal is determined by the bridge detector, amplified, and applied to the lead zirconate titanate (PZT) piezoelectric pushers to return the capacitor plates to position. Because of this servo action, the bridge detector may be operated at maximum sensitivity without being driven beyond its linear range.

The $Pb(Mg_{1/3}Nb_{2/3})O_3$ ceramic sample was driven at 7 Hz without applying a voltage to the standard crystal (Fig. 6a). The expected quadratic relation between voltage and output is clearly evident. Fig. 6b shows an example of the null condition. After proper adjustment of phase with a certain voltage level applied to the sample, the output curve was obtained as a function of voltage applied to the quartz standard. Balance gave the electrostriction coefficient $\bar{M}_{11} = 8.46 \times 10^{-3} d_{11}$ (quartz) or $1.92(\pm 0.02) \times 10^{-16}\,m^2V^{-2}$, in good agreement with the value determined by the strain gauge method [13].

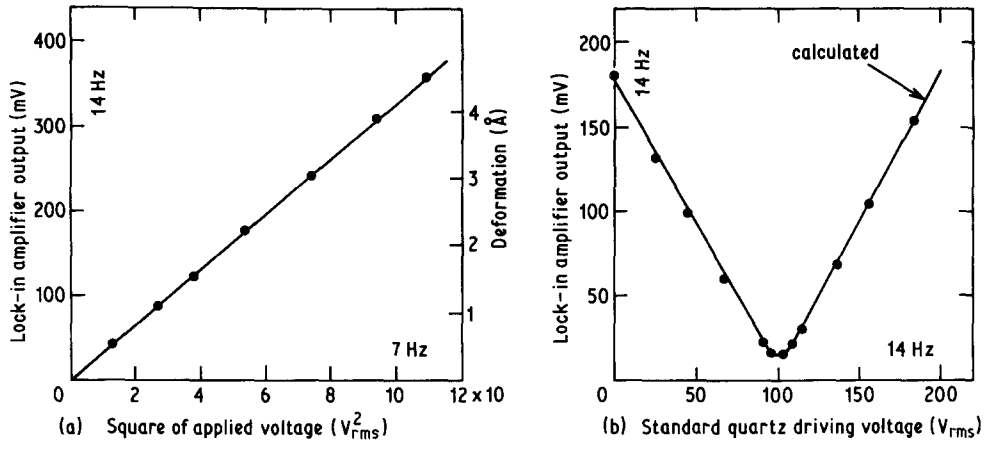

Figure 6 (a) Dilatometer output as a function of square of driving voltage applied to $Pb(Mg_{1/3}Nb_{2/3})O_3$ ceramic; sample thickness = 3.68 mm and C = 74.1 pF. (b) Null condition between $Pb(Mg_{1/3}Nb_{2/3})O_3$ and quartz; PMN driving voltage = 74.7 V_{rms} (7 Hz) and C = 74.0 pF.

5. Electrostriction in perovskite crystals

Hydrostatic electrostriction coefficients Q_h and Curie–Weiss constants C, for several kinds of perovskite type oxide crystals are summarized in Table I. Coefficients are listed for simple, disordered, partially-ordered and ordered ferroelectrics, antiferroelectrics, and non-polar dielectrics. Sources of the original experimental data are listed in references [6, 10, 14]. The magnitude of the electrostrictive coefficient is not effected strongly by ferroelectricity, antiferroelectricity, or non-polar behaviour, but is very dependent on the degree of order in the cation arrangement. It is proposed that "the electrostrictive coefficient Q increases with cation order from disordered, through partially-ordered, simple and then ordered perovskites", is used as an empirical rule i.e. Rule I. The decrease in the Curie–Weiss constant from its highest values in disordered, through partially-ordered, and simple and ordered perovskites is also suggestive. This leads to experimental Rule II, that is, "the product of the electrostriction coefficient, Q, and the Curie-Weiss constant, C, is nearly constant for all ferroelectric and antiferroelectric perovskites ($Q_hC = 3.1(\pm 0.4) \times 10^3 m^4 C^{-2} K$)."

The results of the electrostriction measurements on the solid solution systems are also very suggestive. In the $SrTiO_3$–$Bi_{2/3}TiO_3$ system [14], the substitution of Bi^{3+} for Sr^{2+} causes a remarkable decrease in the electrostriction coefficient from $Q_h = 5.0 \times 10^{-2} m^4 C^{-2}$ in $SrTiO_3$ to $Q_h = 1.3 \times 10^{-2}$ m^4 C^{-2} in 0.856 $SrTiO_3$–0.144 $Bi_{2/3}TiO_3$. In the systems $Pb(Mg_{1/3}Nb_{2/3})O_3$–$PbTiO_3$ [13] and $Pb(Mg_{1/3}Nb_{2/3})O_3$–$Pb(Mg_{1/2}W_{1/2})O_3$ [15], the small Q_h value of $Pb(Mg_{1/3}Nb_{2/3})O_3$ increases

TABLE I Electrostrictive coefficients, Curie–Weiss constants and their product values for various perovskite-type crystals [6, 10, 14]

Polar-type	Order-type	Substance	Q_h ($\times 10^{-2} m^4 C^{-2}$)	C ($\times 10^5$ K)	Q_hC ($\times 10^3 m^4 C^{-2} K$)
Ferroelectric	Disordered	$Pb(Mg_{1/3}Nb_{2/3})O_3$	0.60	4.7	2.8
		$Pb(Zn_{1/3}Nb_{2/3})O_3$	0.66	4.7	3.1
	Partially ordered	$Pb(Sc_{1/2}Nb_{1/2})O_3$	0.83	3.5	2.9
	Simple	$BaTiO_3$	2.0	1.5	3.0
		$PbTiO_3$	2.2	1.7	3.7
		$SrTiO_3$	4.7	0.77	3.6
		$KTaO_3$	5.2	0.5	2.6
Antiferroelectric	Partially ordered	$Pb(Fe_{2/3}U_{1/3})O_3$	–	2.3	–
	Simple	$PbZrO_3$	2.0	1.6	3.2
	Ordered	$Pb(Co_{1/2}W_{1/2})O_3$	–	1.2	–
		$Pb(Mg_{1/2}W_{1/2})O_3$	6.2	0.42	2.6
Non-polar	Disordered	$(K_{3/4}Bi_{1/4})(Zn_{1/6}Nb_{5/6})O_3$	0.55–1.15	–	–
	Simple	$BaZrO_3$	2.3	–	–

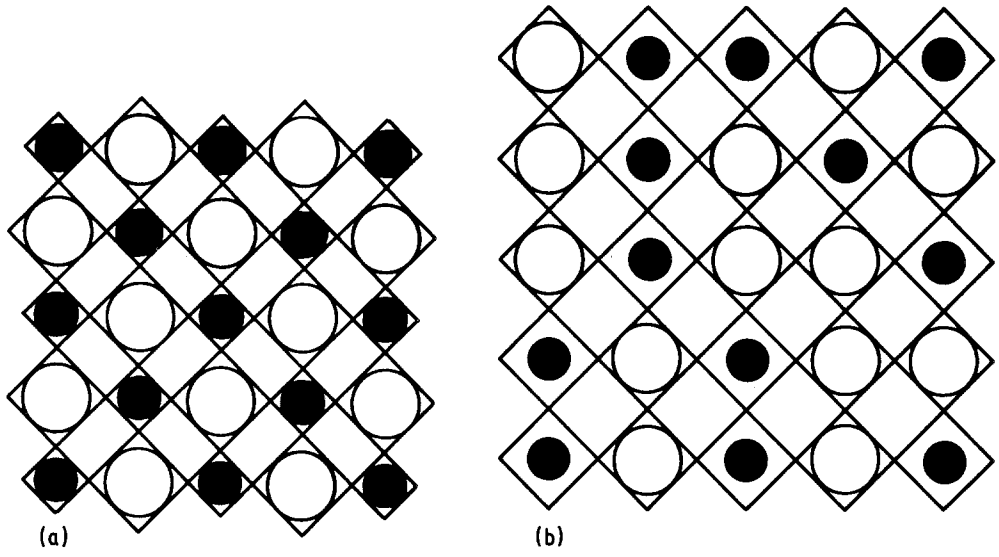

Figure 7 Crystal structure models of the $A(B_{I_{1/2}}B_{II_{1/2}})O_3$ type perovskite: (a) ordered structure with a small rattling space, and (b) disordered structure with a large rattling space. ○ = B_I ion and ● = B_{II} ion.

with increasing $PbTiO_3$ or $Pb(Mg_{1/2}W_{1/2})O_3$ content. A larger rate of increase was observed for the $Pb(Mg_{1/3}Nb_{2/3})O_3$–$Pb(Mg_{1/2}W_{1/2})O_3$ system than for the $Pb(Mg_{1/3}Nb_{2/3})O_3$–$PbTiO_3$ system because of the tendency of Mg and W ions to order.

An intuitive crystallographic model to explain the "constant QC rule" has been proposed. Fig. 7a and b show the ordered and disordered structures for an $A(B_{I_{1/2}}B_{II_{1/2}})O_3$ perovskite crystal. Assuming a rigid ion model, a large "rattling" space is expected for the smaller B ions in the disordered structure because the larger B ions prop open the lattice framework. Much less "rattling" space is expected in the ordered arrangement where neighbouring atoms collapse systematically around the small B ions. The densely-packed structure of B ions in the ordered perovskite illustrated in Fig. 7a has been observed for 0.9 $Pb(Mg_{1/2}W_{1/2})O_3$–0.1 $Pb(Mg_{1/3}Nb_{2/3})O_3$ by Amin *et al.* [16]. When an electric field is applied to a disordered perovskite, the B ions with a large rattling space can shift easily without distorting the oxygen framework. Larger polarization can be expected for unit magnitude of electric field, in other words, larger dielectric constants and larger Curie–Weiss constants. Also smaller strains are expected per unit magnitude of polarization, resulting in lower electrostriction coefficients. On the other hand, in ordered perovskites with a very small rattling space, the B ions cannot move easily without distorting the octahedron. A smaller Curie–Weiss constant and a larger electrostriction coefficient are expected.

6. Giant electrostriction in relaxor ferroelectrics [13, 17]

Since the magnitude of electrostrictive displacement under electric field may be estimated from the value of $Q\epsilon^2$ (ϵ = permittivity) or QC^2 (eliminating the temperature dependence), and the product QC is nearly constant for all ferroelectric perovskites, relaxor (disordered) ferroelectrics with small electrostrictive Q coefficient but very large permittivity (or Curie–Weiss constant), are preferred to the usual perovskites (e.g. Pb(Zr, Ti)O_3 or $BaTiO_3$ based ceramics) for practical applications.

The relaxor ferroelectric chosen for study is $Pb(Mg_{1/3}Nb_{2/3})O_3$, which itself is superior to conventional modified $BaTiO_3$ ceramics in its electrostrictive response. The response can be further improved if the Curie range, which is below room temperature in $Pb(Mg_{1/3}Nb_{2/3})O_3$, could be shifted to a slightly higher temperature. In this section the results for a composition in the $Pb(Mg_{1/3}Nb_{2/3})O_3$–$PbTiO_3$ solid solution series, 0.9 $Pb(Mg_{1/3}Nb_{2/3})O_3$–0.1 $PbTiO_3$ are described.

The Curie range of this sample extends from about 0 to 40° C, and the room temperature dielectric constant is about 7000 at 1 kHz. Using a differential transformer dilatometer, the transverse electrostrictive strain x_2 was measured along the length of a thin ceramic rod, subject to d.c. bias fields (E_1) applied in a perpendicular direction (Fig. 8). The relaxor ceramics are anhysteretic, and

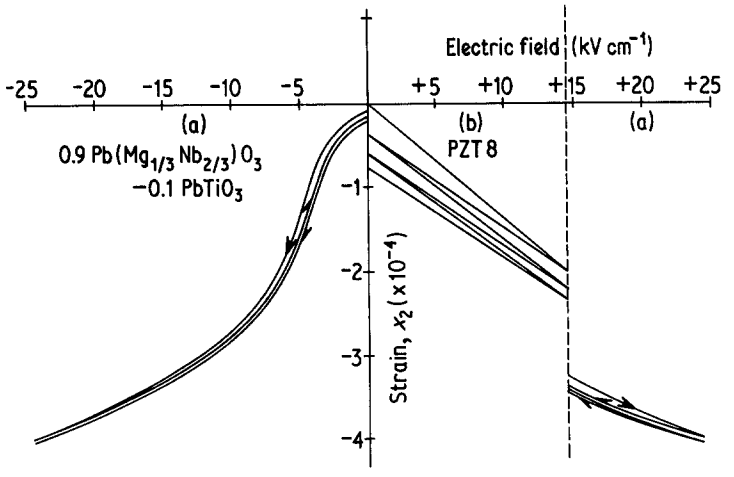

Figure 8 Transverse strain in ceramic specimens of (a) 0.9 $Pb(Mg_{1/3}Nb_{2/3})O_3$–0.1 $PbTiO_3$ and (b) a typical hard PZT 8 piezoceramic under slowly varying electric fields.

retrace the same curve with rising and falling fields. For comparison the piezoelectric strain of a hard PZT 8 under cyclic fields is also plotted in Fig. 8. This material has often been used in the fabrication of multi-dither mirrors and other active optical components [18]. Field-induced strains in 0.9 $Pb(Mg_{1/3}Nb_{2/3})O_3$–0.1 $PbTiO_3$ are larger than those in PZT and far more reproducible under cyclic drive conditions. Transverse electrostrictive strain is defined as $x_2 = \bar{Q}_{12}P_1^2$ where $\bar{Q}_{12}$ is the polycrystalline (averaged) electrostriction coefficient and P_1 the electric polarization induced by an electric field E_1. The strain x_2 is plotted as a function of P_1^2 in Fig. 9. It is evident that the linear relation between x_2 and P_1^2 is substantiated even for high-permittivity materials such as 0.9 $Pb(Mg_{1/3}Nb_{2/3})O_3$–0.1 $PbTiO_3$. The electrostriction coefficient $\bar{Q}_{12}$ calculated from the slope of the line is $-0.9 \times 10^{-2}\,m^4C^{-2}$, which is slightly smaller than other simple perovskites. The large electrostrictive strains of relaxor ferroelectrics can be attributed primarily to the large dielectric constant rather than to a big (electrostrictive) coupling coefficient.

Another interesting property of relaxor ferroelectrics is the very small thermal expansion effect throughout the Curie range, as expected from the empirical rule $\alpha^2 \propto Q$ as discussed in Section 2. Fig. 10 shows the thermal strain of 0.9 $Pb(Mg_{1/3}Nb_{2/3})O_3$–0.1 $PbTiO_3$ plotted as a function of temperature. In the temperature range -100 to $+100^\circ$ C, the thermal expansion coefficient is less than $1 \times 10^{-6}K^{-1}$, comparable to the best low-expansion ceramics or fused silica. The thermal strains (Fig. 10) are far smaller than the electrostrictive strains (Fig. 8), which is extremely advantageous for micropositioner applications, since dimension changes caused by temperature variations ($\Delta L/L \sim \pm 5 \times 10^{-6}$ for $\Delta T \sim \pm 10$ K) can easily be compensated electrically (± 200 V cm^{-1} feedback).

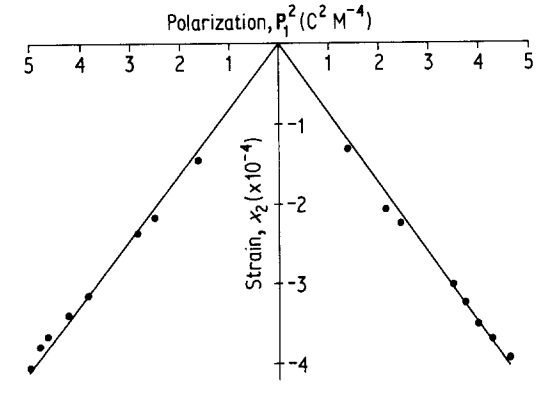

Figure 9 Field-induced transverse strain in ceramic 0.9 $Pb(Mg_{1/3}Nb_{2/3})O_3$–0.1 $PbTiO_3$ plotted against the square of the electric polarization.

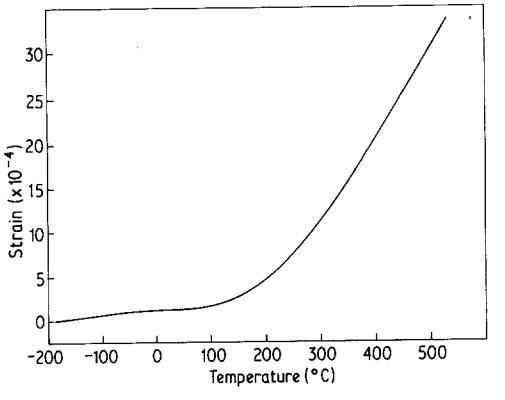

Figure 10 Thermal expansion in polycrystalline 0.9 $Pb(Mg_{1/3}Nb_{2/3})O_3$–0.1 $PbTiO_3$.

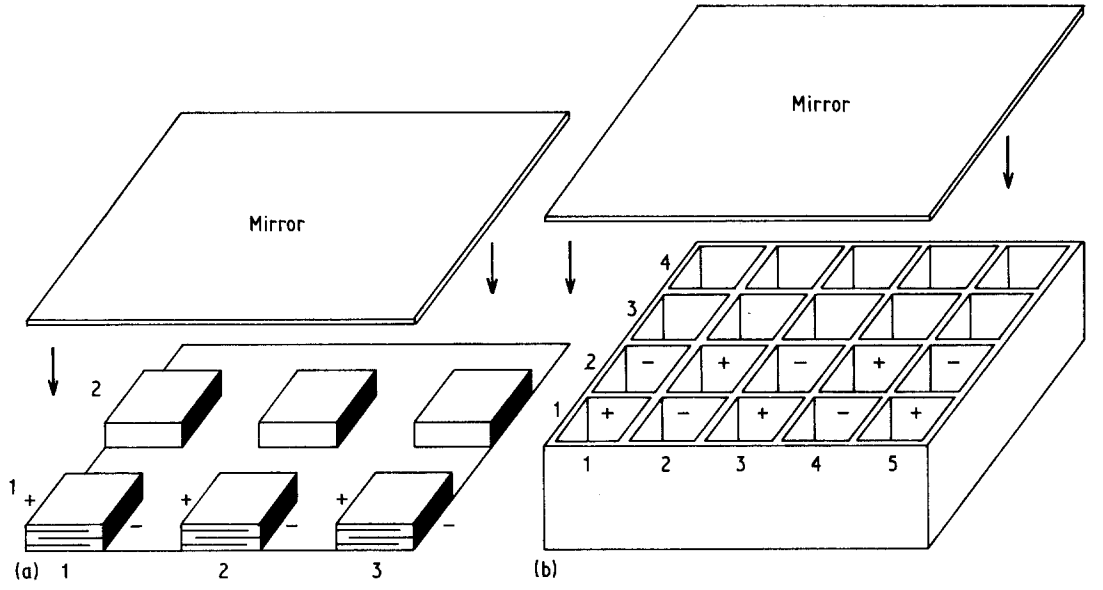

Figure 11 Device arrangements for mirror control application: (a) a multilayer type (longitudinal effect device) and (b) a honeycomb-type (transverse effect device).

7. New mirror-control devices [19]

The multilayer technology used in the capacitor industry is one of the important factors prompting the development of new electrostrictive devices. Fig. 11a shows the basic internal-electrode configuration used in displacement transducers. The electric field across alternate layers is of opposite direction, but the displacive responses are additive. In a piezoelectric device of fixed total thickness, the total displacement for a given voltage is proportional to the number of layers. On the other hand, in an electrostrictive device the total displacement is proportional to the *square* of the number of layers, more effective than in a piezoelectric material.

Internally-electroded multiplayer samples were prepared by standard tape-casting techniques using calcined $0.9\,Pb(Mg_{1/3}Nb_{2/3})O_3$–$0.1\,PbTiO_3$ powder and a commercial doctor blade media (Cladan Inc., San Diego, CA, type B42). Internal electrodes were applied by screen printing platinum ink (Englehard industries, East Newark, NJ, type E-305-A) onto the dried cast tape. Detailed procedures are described in the paper of Bowen *et al.* [20]. Ten-layer devices with a total thickness of 2.5 mm were prepared by firing on platinum setters in air at 1000° C for 2 h.

Compared with the electrostriction data for simple plate devices in Section 6, the strain of the multilayer devices was smaller than expected, which can be attributed to the effect of the multilayer configuration. Two separate electrode systems and the insulated electrode edges reduce the measured displacement [20].

Notwithstanding this clamping effect, a mirror control device has been constructed from *ten* ten-layer ceramics bonded together. With only 200 V applied, the device develops large displacements up to $\Delta L \sim 25\,\mu m$ ($\Delta L/L \sim 10^{-3}$) with very high reproducibility under cyclic fields. The dimension change associated with a temperature variation of 10 K was less than 0.4 μm. With further refinement of the tape casting process, it is probable that the driving voltage can be further reduced to less than 40 V. The total displacement of about 25 μm is an order of magnitude larger than that of the commercial piezoelectric transducers [21] (e.g. PZT-5H, 25 mm plate using d_{31}), and may introduce a new class of micropositioner devices.

Fig. 11a and b show the device arrangements for practical mirror-control applications. Fig. 11a is an example using the multilayer devices (longitudinal effect device) and Fig. 11b is a honeycomb-type displacement device which is manufactured by an extrusion technique, and electroded inside the tubes (transverse effect device). Voltages applied to each address (element) leads to localized mirror control.

8. Summary

From intensive studies on the electrostrictive effects in ferroelectric, antiferroelectric and non-

polar perovskites, several empirical rules have been found:

(a) The magnitude of the electrostrictive coefficient Q is not effected strongly by ferroelectricity, antiferroelectricity or non-polar behaviour, but is very dependent on the degree of order in the cation arrangement. The Q value increases with cation order from disordered, though partially-ordered to simple and then ordered perovskites.

(b) The product of the electrostriction coefficient Q and the Curie–Weiss constant C is nearly constant for all ferroelectric and antiferroelectric perovskites ($Q_h C = 3.1\ (\pm 0.4) \times 10^3\ m^4\ C^{-2}\ K$).

(c) The value of the electrostriction coefficient Q is approximately proportional to the square of the thermal expansion coefficient α ($\alpha = 4.2 \times 10^{-5}\ Q_h^{0.5}$).

Relaxor ferroelectrics offer several advantages over normal piezoelectric transducers:

(1) Large electrostrictive strains comparable to the best piezoelectric ceramics.

(2) Excellent positional reproducibility.

(3) No poling is required.

(4) Very low thermal expansion coefficients.

Using the multilayer configuration of existing capacitor technology with the ceramic 0.9 $Pb(Mg_{1/3}Nb_{2/3})O_3$–0.1 $PbTiO_3$, a mirror control device which can develop a large strain with high reproducibility, up to $\Delta L/L \sim 10^{-3}$ when only 200 V is applied has been developed.

In the inverse electrostrictive effect, that is, the pressure dependence of dielectric constant, a sensitive pressure characteristic has also been observed in the same material. Applications of this electrostrictive material for pressure gauges, water-depth meters and heavy-weight detectors are also very promising [22].

References

1. K. UCHINO and L. E. CROSS, *Japan. J. Appl. Lett.* **19** (1980) L171.
2. A. F. DEVONSHIRE, *Phil. Mag. Suppl.* **3** (1954) 85.
3. H. F. KAY, *Rep. Prog. Phys.* **43** (1955) 230.
4. P. W. FORSBERGH, Jr. "Handbuch der Physik", Vol. 17, (Springer-Verlag, Berlin, 1956) p. 264.
5. C. KITTEL, *Phys. Rev.* **82** (1951) 729.
6. K. UCHINO, L. E. CROSS, R. E. NEWNHAM and S. NOMURA, *J. Appl. Phys.* **8** (1980) 4356.
7. L. E. CROSS, *J. Phys. Soc. Japan* **23** (1967) 77.
8. G. A. SAMARA, *Phys. Rev.* **B1** (1970) 3777.
9. I. N. POLANDOV, *Sov. Phys.-Sol. Stat.* **5** (1963) 838.
10. K. UCHINO, S. NOMURA, L. E. CROSS, S. J. JANG and R. E. NEWNHAM, *J. Appl. Phys.* **51** (1980) 1142.
11. K. UCHINO and L. E. CROSS, Proceedings 33rd Annual Symposium on Frequency Control, US Army Electronics Command, Fort Monmouth, NJ (1979) 110.
12. *Idem, Ferroelectrics* **27** (1980) 35.
13. S. J. JANG, K. UCHINO, S. NOMURA and L. E. CROSS, *ibid.* **27** (1980) 31.
14. K. UCHINO, L. E. CROSS, R. E. NEWNHAM and S. NOMURA, *J. Phase Transitions* **1** (1980) 333.
15. S. NOMURA, J. KUWATA, K. UCHINO, S. J. JANG, L. E. CROSS and R. E. NEWNHAM, *Phys. Stat. Sol. (a)* **57** (1980) 317.
16. A. AMIN, R. E. NEWNHAM, L. E. CROSS, S. NOMURA and D. E. COX, *J. Sol. State. Chem.* **35** (1980) in press.
17. L. E. CROSS, S. J. JANG, R. E. NEWNHAM, S. NOMURA and K. UCHINO, *Ferroelectrics* **23** (1980) 187.
18. J. FEINLEIB, S. G. LIPSON and P. F. CONE, *Appl. Phys. Lett.* **25** (1974) 311.
19. K. UCHINO, L. E. CROSS and S. NOMURA, *J. Mater. Sci.* **15** (1980) 2643.
20. L. J. BOWEN, T. SHROUT, W. A. SCHULZE and J. V. BIGGERS, *Ferroelectrics* **27** (1980) 59.
21. R. A. LEMONS and L. A. COLDREN, *Rev. Sci. Instrum.* **49** (1978) 1650.
22. K. UCHINO, S. J. JANG, L. E. CROSS and R. E. NEWNHAM, USA Patent disclosure 80-461. Pressure gauge using relaxor ferroelectric.

Received 24 July and accepted 8 October 1980.